NUMERICAL SIMULATION OF THERMAL PERFORMANCE OF CONSTANT CONDUCTANCE CYLINDRICAL HEAT PIPE USING NANOFLUID

Hassanain Ghani Hameed
Foundation of Technical Education
Engineering Technical College/ Najaf
Automobile Department
hasgh77@yahoo.com

Proof. Dr. Abudl-Muhsin A. Rageb
University of Basra
Engineering College
Mechanical Engineering Department
Muhsin Rageb@yahoo.ie

Received 6 June 2014 Accepted 1 September 2014

ABSTRACT

In this work, a two-dimensional numerical model has been developed to study the thermal performance of a cylindrical heat pipe utilizing nanofluids. Al_2O_3-water based is considered as the working fluid. The numerical model represented as steady-state incompressible flow. The governing equations in cylindrical coordinates have been solved in vapor region, wick structure and wall region, using finite deference with forward-backward upwind scheme. A substantial change in the heat pipe liquid pressure drop, temperature difference, maximum heat transfer limit, capillary pressure and thermal resistance is observed when using a nanofluid. The nanoparticles within the liquid enhance the thermal performance of the heat pipe by reducing the thermal resistance and temperature difference by 0.168 K/W and 5.06 K respectively. While increasing the maximum heat load and the capillary pressure by 96 W and 192.46 Pa respectively. All these results at input heat of 30 W and nanoparticles concentration of 5 Vol. %.The results of wall temperature distribution for the heat pipe have been compared with the previous study for the same problem and a good agreement has been achieved.

KEYWORDS: Cylindrical heat pipe; Nanofluid; Numerical simulation.

حسنين غني حميد
هيئة التعليم التقني
الكلية التقنية الهندسية / النجف
قسم هندسة تقنيات السيارات

أ.د. عبد المحسن عبود رجب
جامعة البصرة
كلية الهندسة
قسم الهندسة الميكانيكية

الخلاصة:

في هذا البحث, تم تطوير نموذج عددي ثنائي البعد لدراسة الاداء الحراري لأنبوب حراري اسطواني باستخدام المائع الدقيق (النانوفلود) نوع الالومينا المخلوط بالماء. تم تمثيل النموذج العددي بالجريان اللانضغاطي في الحالة المستقرة. تم حل المعادلات الحاكمة بصيغة الاحداثيات الاسطوانية في منطقة البخار, تركيب الفتيل ومنطقة الجدار باستخدام طريقة الفروقات المحددة مع نظام أمام- خلف مع الريح. تم ملاحظة تغير حقيقي في هبوط الضغط, فرق درجة الحرارة, حد انتقال الحرارة الاعظم, الضغط الشعري و المقاومة الحرارية للانبوب الحراري عند استخدام مائع دقيق. وجود الدقاق النانوية ضمن المائع يعزز الاداء الحراري للانبوب عن طريق تقليل المقاومة الحرارية وفرق درجة الحرارة نحو 0.168 K/W و 5.06 K على التوالي. بينما يزيد الحمل الحراري الاعظم و الضغط الشعري نحو 96 W و 192.46 Pa على التوالي. حيث ان كل هذه النتائج عند كمية حرارة 30 W و تركيز

الجزيئات الدقيقة .% Vol. 5. تم مقارنة النتائج الخاصة بتوزيع درجات على جدار الانبوب الحراري مع الدراسات السابقة وكان هنالك توافق جيد.

NOMENCLATURE

A = area (m^2)
C_p = heat capacity at constant pressure (kJ/kg. K)
Da = Darcy number
h = convective heat transfer coefficient (W/m^2 . K)
h_{fg} = latent heat of vaporization (kJ/kg)
k = thermal conductivity (W/m. K)
k_{eff} = effective thermal conductivity of the liquid-saturated wick (W/m. K)
K_p = permeability of the wick (m^2)
L = length (m)
L_{eff} = effective length of heat pipe (m)
P = pressure (N/m^2)
Q = heat transfer (W)
r = redial coordinate (m)
r_c = capillary radius of wick (m)
R = gas constant (kJ/kg. K)
R_{th} = thermal resistance (K/W)
Re = Reynolds number
Pr = prandtl number
T = temperature (K)
u = axial velocity (m/sec)
v = radial vapor velocity (m/sec)
V = reference velocity (m/sec)
x = axial coordinate (m)

Greek Symbols

ε = porosity of the wick
φ = nanoparticle concentration
Ψ = stream function (m^3/sec)
ω = vorticity (sec^{-1})
α = fluid thermal diffusivity (m^2/sec)
υ = kinematics viscosity (m^2/sec)
μ = dynamic viscosity (kg/m. sec)
σ = surface tension (N/m)
ρ = density (kg/m^3)
β = inclination angle of heat pipe
θ = dimensionless temperature

Subscripts

***** = dimensionless term
a = adiabatic
c = condenser
col = coolant
e = evaporator
f = base fluid
in = inlet
int = interface
l = liquid
n = nanofluid
o = outer
p = particle
s = sink, solid
sat = saturated
set = set point
v = vapor
w = wick
wa = wall

Superscripts

$\bar{}$ = average quantity

1. INTRODUCTION

Heat pipes have been the center of attention as high heat transfer devices for a couple of decades. During the time of heat pipe development two approaches have been followed in order to enhance the heat pipe heat transfer capacity and reduce its thermal resistance. One approach is to improve heat pipes' structure including the pipe modification – e.g. using finned pipes, annular structure – and wick modification – e.g. new wick designs or wicks combinations. Another approach is to seek better working fluids which are compatible with the heat pipe structure and have higher thermal properties.

A novel idea, by applying nanofluids as working fluids in heat pipes, that can be found only in the literature of the last decade. This idea enhance the maximum heat transport rate and the effective thermal resistance which represent the main parameters that characterize the thermal performance of a wicked heat pipes **(Hajian et. al 2012, Peterson 1994).**

(Do et al. 2010) experimentally, investigated the effects of the water-based Al_2O_3 nanofluids on the thermal performance of heat pipes with the volume fraction of 1.0 and 3.0 Vol.%. Based on the experimental results it is shown that the utilization of the water- based Al_2O_3 nanofluids as the working fluid enhances the thermal performance of the heat pipe and the volume fraction of nanoparticles has a great effect on the reduction of the wall temperature at the evaporator section. The thermal resistance of the heat pipe using the water-based Al_2O_3 nanofluids with 3.0 Vol.% is significantly decreased up to about 40% at the evaporator-adiabatic section as compared with that of the distilled (DI) water-based heat pipe. Also, it is shown that the maximum heat transfer rate of the heat pipes can be enhanced using the water-based Al_2O_3 nanofluids instead of DI water.

(Mousa 2011), presented an experimental study for the behavior of nanofluid to improve the performance of a circular heat pipe. Pure water and Al_2O_3-water based nanofluid are used as working fluids. The effect of filling ratio, volume fraction of nanoparticles in the base fluid, and heat input rate on the thermal resistance is investigated. Total thermal resistance of the heat pipe for pure water and Al_2O_3-water based nanofluid is also predicted. An experimental correlation is obtained to predict the influence of Prandtl number and dimensionless heat transfer rate, Kq on thermal resistance. Thermal resistance decreases with increasing Al_2O_3-water based nanofluid compared to that of pure water.

An experimental study was performed to investigate the thermal performance of an inclined miniature mesh heat pipe using water-based CuO nanofluid as the working fluid by (**Wang et al 2012)**. The study focused mainly on the effects of the inclination angle and the operating temperature on the heat transfer performance of the heat pipe using the nanofluid with the mass concentration of CuO nanoparticles of 1.0 wt%. The experiment was performed at three steady operating temperatures of 40°C, 50°C and 60°C. Experimental results show that the inclination angle has a strong effect on the heat transfer performance of heat pipes using both water and the nanofluid. The inclination angle of 45 ° corresponds to the best thermal performance for heat pipes using both water and the nanofluid.

(Liu 2011) performed an experiment concerning a cylindrical mesh wicked heat pipe. The working fluid was an aqueous CuO nanofluids. The results show that adding CuO nanoparticles into deionized water with concentration of 1.0 wt.% can enhance the evaporating heat transfer coefficient averagely 2.5 times, and the maximum heat flux of the heat pipe enhance by 42%.

(Naphon et al. 2008) investigated titanium–alcohol nanofluid effects on heat pipe thermal performance, for different working fluid charging amount, heat pipe tilt angle and nanoparticles volume concentrations. They found that nanoparticles enhance the heat pipe thermal performance.

(Tsai et al. 2004) used a circular meshed heat pipe with 170 mm length and 6 mm of outer diameter to investigate effects of structural character of gold nanoparticles in nanofluid on heat pipe thermal performance. They found that, there is a significant reduction in thermal resistance of heat pipe with nanofluids solution as compared with DI-water. Also the results show that the thermal resistance of a vertical meshed heat pipe varies with the size of gold nanoparticles.

An experimental investigation is carried out by **(Solomon et al 2012)** to study the thermal performance of a heat pipe operated with nanoparticle coated wick. The thermal resistance and heat transfer coefficient in the evaporator of the heat pipe operated with coated wick are lower and higher respectively than that of conventional one whereas the same are opposite in the condenser at three different heat inputs. The total resistance of heat pipe operated with coated wick is lower than that of conventional one and it decreases with increasing heat input. At the evaporator section, 40% thermal resistance reduction and 40% heat transfer coefficient enhancement are observed.

(Kang et al. 2006) investigated the effects of silver nanofluid on grooved circular heat pipe with 200 mm length and 6 mm diameter. They observed 10–80% decrease in thermal resistance of the heat pipe compared to DI-water at an input power of 30-60 watt. The results also show that the thermal resistances of the heat pipe decrease as the silver nanoparticle size and concentration increase.

(Kang et al. 2009) used a sintered heat pipe to investigate effects of an aqueous solution of 10 and 35 nm diameter silver nanoparticles and its concentration on heat pipe thermal performance. Their experiments demonstrated that the temperature difference decreased 0.56-0.65 ^{o}C compared to DI-water at an input power of 30-60 W, and also heat transfer capacity of heat pipe increased from 50 W by using DI-water to 70 W by using nanofluid as a working fluid.

The transient and steady state thermal performances of a medium-sized cylindrical stainless steel meshed heat pipe have been investigated experimentally by **(Hajian 2012)**, utilizing both DI-water and silver nanofluid, as the working fluids. The experiments have been performed under heat rates in the medium range, less than 500 W. Nanofluids were used with concentrations of 50, 200 and 600 ppm. By applying 50 ppm nanofluid, the thermal resistance and the response time of the heat pipe decreased by 30% and about 20%, respectively, compared to DI-water. Furthermore, the steady state performance of both DI-water and nanofluid were better at higher heat rates, about 500 W. Whereas 50 ppm nanofluid, as the working fluid, enhanced the thermal performance of the heat pipe in comparison with DI-water, the nanofluids with more concentration did not.

In an analytical study about nanofluid performance in heat pipe, **(Shafahi et al. 2010)**, used two-dimensional analysis to study the thermal performance of heat pipe utilizing nanofluids. Their analysis was based on a comprehensive analytical model which was proposed by (**Zhu and Vafai 1999)**. They considered nanoparticles Al_2O_3, CuO, and TiO_2 in their study and investigated the effect of these nanoparticles on thermal resistance, temperature distribution, and maximum capillary heat transfer (MCHT) of heat pipe. They observed reduction in the thermal resistance and enhancing the MCHT of heat pipe. They established an optimum mass concentration for nanoparticles in maximizing the heat transfer limit. They also investigated the effect of particle size on the heat pipe performance and found that smaller nanoparticles have more effects on temperature gradient along the heat pipe.

A mathematical model was developed by **(Do 2010)**, for quantitatively evaluating the thermal performance of a water-based Al_2O_3 nanofluid heat pipe with a rectangular grooved wick. The results show that at the optimum conditions, the thermal performance for the nanofluid heat pipe was significantly enhanced by about 100% when only a small amount of nanoparticles less than 1.0 vol% is added into the base fluid. Also, the thermal resistance of the nanofluid heat pipe tended to decrease with increasing the nanoparticle size. The heat transfer enhancement ratio ranged from 1.2 to 2.2 for the different nanoparticle size, working temperature, and input heat rate. From the comparison of the thermal performance using both DI water and nanofluids, it is found that the thin porous coating layer formed by nanoparticles suspended in nanofluids is a key effect of the heat transfer enhancement for the heat pipe using nanofluids.

In this paper a numerical model has been developed to study the effect of Al_2O_3-water based nanofluid (as working fluid), volume fraction of nanoparticles in the base fluid, and heat input rate on the thermal performance of a heat pipe. The steady state incompressible flow has been solved in cylindrical coordinates in vapor region, wick structure and wall region, using finite difference method. The Darcy's law has been employed for momentum equation in porous media. The governing equations have been solved using upwind scheme.

2. MATHEMATICAL MODEL

A cylindrical heat pipe as shown in **Fig. 1** consists of three main parts, namely evaporator section, adiabatic section and condenser section.

External heat source applied at the evaporator section causes vaporization of the working liquid. Due to the pressure gradient, the vapor flows to the condenser section and it condenses when the heat removed from the condenser wall surface by free or forced convection. The capillary pressure created by the wick structure, pumps the condensed fluid back to the evaporator. This process will continue as long as there is sufficient capillary pressure to drive the condensate back to the evaporator.

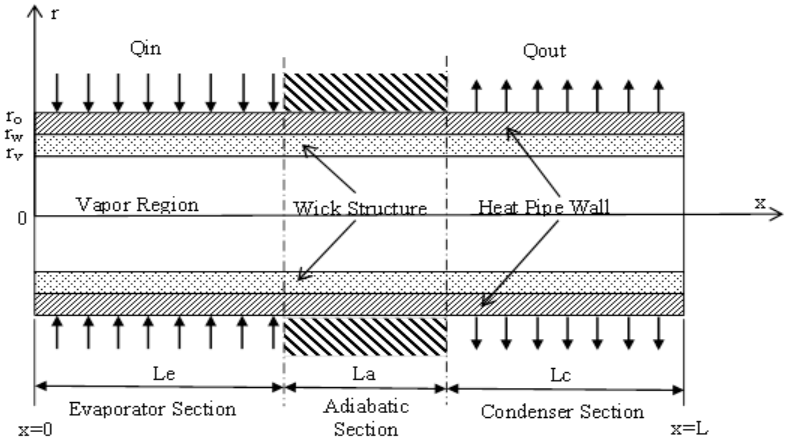

Figure 1: Schematic of a cylindrical heat pipe under consideration.

2.1 GOVERNING EQUATIONS AND BOUNDARY CONDITIONS

The steady state incompressible laminar flow has been solved in cylindrical coordinates in vapor region, wick structure and wall region. The wick is assumed isotropic and saturated with the working liquid. The vapor injection and suction at the liquid-vapor interface are assumed to be uniform.

2.1.1 Vapor Region

The governing equations in vapor region are continuity, Navier-Stokes and energy equations as follows, **(Jiji 2006)**:

$$\frac{\partial u}{\partial x}+\frac{1}{r}\frac{\partial (rv)}{\partial r}=0 \qquad (1)$$

$$\rho_n u\frac{\partial u}{\partial x}+\rho_n v\frac{\partial u}{\partial r}=-\frac{\partial p}{\partial x}+\mu_n\left[\frac{\partial^2 u}{\partial x^2}+\frac{1}{r}\frac{\partial u}{\partial r}+\frac{\partial^2 u}{\partial r^2}\right] \qquad (2)$$

$$\rho_n u\frac{\partial v}{\partial x}+\rho_n v\frac{\partial v}{\partial r}=-\frac{\partial p}{\partial r}+\mu_n\left[\frac{\partial^2 v}{\partial x^2}+\frac{1}{r}\frac{\partial v}{\partial r}+\frac{\partial^2 v}{\partial r^2}-\frac{v}{r^2}\right] \qquad (3)$$

$$\left(\rho C_p\right)_n\left[u\frac{\partial T}{\partial x}+v\frac{\partial T}{\partial r}\right]=k_n\left[\frac{\partial^2 T}{\partial x^2}+\frac{1}{r}\frac{\partial T}{\partial r}+\frac{\partial^2 T}{\partial r^2}\right] \tag{4}$$

The boundary conditions for vapor region are as following.
The radial velocities at liquid-vapor interface **(Borujerdi and Layeghi 2004)**:

$$\begin{cases} v_e = +\dfrac{Q_e}{2\pi r_v L_e \rho_n h_{fgn}} & 0 \le x \le L_e \\ v_a = 0 & L_e \le x \le L_e + L_a \\ v_c = -\dfrac{Q_c}{2\pi r_v L_c \rho_n h_{fgn}} & L_e + L_a \le x \le L_e + L_a + L_c \end{cases} \tag{5}$$

The temperature at the vapor-liquid interface of the evaporator and condenser is calculated approximately using Clausius-Clapeyron equation, **(Borujerdi and Layeghi 2004).**

$$T_{\text{int}} = \frac{1}{\dfrac{1}{T_{nv,sat}} - \dfrac{R_n}{h_{fg}}\ln\dfrac{P_{nv}}{P_{nv,sat}}} \tag{6}$$

The boundary conditions at both pipe ends are:

$$v = u = 0 \qquad \frac{\partial T}{\partial x} = 0 \tag{7}$$

At pipe centerline the symmetry boundary conditions are:

$$v = 0, \qquad \frac{\partial u}{\partial r} = 0 \quad \& \quad \frac{\partial T}{\partial r} = 0 \tag{8}$$

2.1.2 Wick Structure

The governing equations in wick structure are as follows, **(Fadhil 2006, Mahjoub and Mahtabroshan 2008)**:

$$\frac{\partial u}{\partial x}+\frac{1}{r}\frac{\partial (rv)}{\partial r}=0 \tag{9}$$

The Darcy's law has been employed for momentum equation in porous media:

$$\rho_n u\frac{\partial u}{\partial x}+\rho_n v\frac{\partial u}{\partial r}=-\frac{\partial p}{\partial x}+\mu_n\left[\frac{\partial^2 u}{\partial x^2}+\frac{1}{r}\frac{\partial u}{\partial r}+\frac{\partial^2 u}{\partial r^2}\right]-\frac{\varepsilon\mu_n}{K_p}u-\frac{\varepsilon^2 F}{K_p^{1/2}}\rho_n|u|u \quad (10)$$

$$\rho_n u\frac{\partial v}{\partial x}+\rho_n v\frac{\partial v}{\partial r}=-\frac{\partial p}{\partial r}+\mu_n\left[\frac{\partial^2 v}{\partial x^2}+\frac{1}{r}\frac{\partial v}{\partial r}+\frac{\partial^2 v}{\partial r^2}-\frac{v}{r^2}\right]-\frac{\varepsilon\mu_n}{K_p}v-\frac{\varepsilon^2 F}{K_p^{1/2}}\rho_n|v|v \quad (11)$$

$$(\rho C_p)_{eff}\left[u\frac{\partial T}{\partial x}+v\frac{\partial T}{\partial r}\right]=k_{eff}\left[\frac{\partial^2 T}{\partial x^2}+\frac{1}{r}\frac{\partial T}{\partial r}+\frac{\partial^2 T}{\partial r^2}\right]+S \quad (12)$$

F is a geometric function based on the porous wick structure and is calculated as follows, (**Zhu and Vafai 1999)**:

$$F=1.75/\sqrt{150}\,\varepsilon^{3/2} \quad (13)$$

The effective thermal conductivity and heat capacity of wick structure, is calculated from equation for screen wire mesh, **(Fadhil 2006, Rashidian 2008)**.

$$k_{eff}=\frac{k_n[(k_n+k_s)-(1-\varepsilon)(k_n+k_s)]}{[(k_n+k_s)+(1-\varepsilon)(k_n-k_s)]} \quad (14)$$

$$(\rho C_p)_{eff}=\varepsilon(\rho C_p)_n+(1-\varepsilon)(\rho C_p)_s \quad (15)$$

The effective thermal conductivity, heat capacity and viscosity for a mixture (nanofluid) with spherical particles is given by **(Shahi 2010, Ferrouillat 2011)**:

$$k_n=\frac{k_f[k_p+2k_f-2(k_f-k_p)\varphi]}{[k_p+2k_f+2(k_f-k_p)\varphi]} \quad (16)$$

$$(\rho C_p)_n=(1-\varphi)(\rho C_p)_f+(\varphi)(\rho C_p)_p \quad (17)$$

$$\mu_n=\frac{\mu_f}{(1-\varphi)^{2.5}} \quad (18)$$

The latent heat of vaporization of Al_2O_3-water based nanofluid with 1, 3, and 5 Vol.% concentration and 25 ±5 nm spherical particles for temperature range of 20-96 ^oC are measured experimentally and represented by the following equations:

$$h_{fgn} = h_{fgf}\left(-119.19\,\varphi^2 + 15.271\,\varphi + 1\right) \tag{19}$$

While, the surface tension of Al_2O_3-water based nanofluid with the same above specifications for temperature range of 20-90 ^oC are measured experimentally and represented by the following equations:

$$\sigma_n = \sigma_f\left(18.934\,\varphi^2 + 1.8266\,\varphi + 1\right) \tag{20}$$

Since the phase change phenomena was not included in current model, for modeling latent heat of vaporization a heat sink was employed in evaporator section and a heat source was used in condenser section. The values of these terms are, **(Mahjoub and Mahtabroshan 2008)**:

$$\begin{cases} S_e = -\dfrac{Q_e}{\pi(r_w^2 - r_v^2)L_e} \\ S_a = 0 \\ S_c = +\dfrac{Q_c}{\pi(r_w^2 - r_v^2)L_c} \end{cases} \tag{21}$$

The boundary conditions at both pipe ends are:

$$v = u = 0 \qquad \frac{\partial T}{\partial x} = 0 \tag{22}$$

The radial blowing and suction velocities at liquid-vapor interface **(Fadhil 2006)**:

$$\begin{cases} v_e = -\dfrac{Q_e}{2\pi r_v L_e \rho_n h_{fgn}\,\varepsilon} & 0 \le x \le L_e \\ v_a = 0 & L_e \le x \le L_e + L_a \\ v_c = +\dfrac{Q_c}{2\pi r_v L_c \rho_n h_{fgn}\,\varepsilon} & L_e + L_a \le x \le L_e + L_a + L_c \end{cases} \tag{23}$$

The temperature at the liquid - vapor interface of the evaporator and condenser is calculated approximately using Clausius-Clapeyron equation, as shown previously in equation (6).

The boundary conditions at both pipe ends are:

$$v = u = 0 \qquad \frac{\partial T}{\partial x} = 0 \tag{24}$$

At wick-wall interface:

$$\begin{cases} k_{eff}\dfrac{\partial T_n}{\partial r} = k_{wa}\dfrac{\partial T_{wa}}{\partial r} \\ T_n = T_{wa} \end{cases} \quad (25)$$

2.1.3 Wall Region

At heat pipe wall the equation of thermal conduction was used in cylindrical coordinates, **(Mahjoub and Mahtabroshan 2008)**:

$$\left[\frac{\partial^2 T_{wa}}{\partial x^2} + \frac{1}{r}\frac{\partial T_{wa}}{\partial r} + \frac{\partial^2 T_{wa}}{\partial r^2}\right] = 0 \quad (26)$$

The boundary conditions in this region are as following:
At both ends of heat pipe:

$$\frac{\partial T_{wa}}{\partial x} = 0 \quad (27)$$

At wall-wick interface, the boundary condition as in equation (25).
At heat pipe external surface:

$$\begin{cases} k_{wa}\dfrac{\partial T_{wa}}{\partial r} = +\dfrac{Q_e}{2\pi r_o L_e} & 0 \le x \le L_e \\ \dfrac{\partial T_{wa}}{\partial r} = 0 & L_e \le x \le L_e + L_a \\ k_{wa}\dfrac{\partial T_{wa}}{\partial r} = -h\left(T_o - T_s\right) & L_e + L_a \le x \le L_e + L_a + L_c \end{cases} \quad (28)$$

In conventional heat pipes, under steady-state operation, there exists a maximum capillary pressure that can be developed in wick structure. The maximum heat transport capillary limit for a heat pipe is achieved when the sum of the pressure losses along the circulation path of the working fluid reaches the maximum capillary pressure; that is

$$\Delta p_{cap} = \Delta p_v + \Delta p_n + \Delta p_g = \frac{2\cos\theta\,\sigma_n}{r_c} \quad (29)$$

Δp_v can be neglecting, can substitute for pressure terms in equation (29), **(Reay 2006)**.

$$\frac{2\cos\theta\,\sigma_n}{r_c}=\left(\frac{\mu_n}{\rho_n}\right)\left(\frac{L_{eff}\,\dot{m}_{\max}}{A_w K_p}\right)+\rho_n g L_{eff}\,\sin\beta \tag{30}$$

$$L_{eff}=\frac{1}{2}\left(L_e+2L_a+L_c\right) \tag{31}$$

For water- based nanofluid as working fluid and horizontal heat pipe the maximum liquid flow rate in the wick become:

$$\dot{m}_{\max}=\left(\frac{\rho_n A_w K_p}{\mu_n L_{eff}}\right)\left(\frac{2\sigma_n}{r_c}\right) \tag{32}$$

Thus, the maximum heat transport capillary limit may be written as, **(Reay 2006)**:

$$Q_{\max}=\dot{m}_{\max}\,h_{fgn}$$

$$Q_{\max}=\left(\frac{\rho_n A_w K_p h_{fgn}}{\mu_n L_{eff}}\right)\left(\frac{2\sigma_n}{r_c}\right) \tag{33}$$

The saturation temperature inside the heat pipe can be calculated from the following equation, **(Cleary 2006)**:

$$T_{sat}=\left(\frac{Q_c}{Q_{\max}}\right)\left(T_{set}-T_s\right)+T_s \tag{34}$$

The thermal resistance, which represent the effectiveness of the heat pipe can be calculated from the following equation, **(Sreenivasa 2005)**:

$$R_{th}=\frac{\overline{T}_e-\overline{T}_c}{Q_{in}} \tag{35}$$

3. METHOD OF SOLUTION

The governing equations are discretized using a finite difference approach and the equations are solved using Forward – Backward upwind with collocated grid scheme. The physical domain of problem was separated into three main regions, namely; vapour region, wick structure and wall region.

It is convenient, For the numerical analysis, to use the governing equations in terms of stream function and vorticity as:

$$u=\frac{1}{r}\frac{\partial\psi}{\partial r} \tag{36}$$

$$v = -\frac{1}{r}\frac{\partial \psi}{\partial x} \tag{37}$$

$$\omega = \frac{\partial v}{\partial x} - \frac{\partial u}{\partial r} \tag{38}$$

Now, after obtained the governing equations in terms of stream function and vorticity ,then they with the corresponding boundary conditions are transferred to the non-dimensional form using the following dimensionless quantities:

$$x^* = \frac{x}{r_o};\ r^* = \frac{r}{r_o};\ u^* = \frac{u}{V};\ v^* = \frac{v}{V};\ \psi^* = \frac{\psi}{Vr_o^2};\ \omega^* = \frac{\omega r_o}{V}$$

$$p^* = \frac{p}{\frac{1}{2}\rho V^2}\ ;\ \theta = \frac{T - T_s}{T_{sat} - T_s}\ ;\ \mathrm{Pr} = \frac{\mu C_p}{k}\ ;\ \mathrm{Re} = \frac{Vr_v}{\upsilon} \tag{39}$$

$$\rho^* C_p^* = \frac{\left(\rho C_p\right)_n}{\left(\rho C_p\right)_f} = 1 - \varphi + \varphi\frac{\left(\rho C_p\right)_p}{\left(\rho C_p\right)_f};\ \mu^* = \frac{\mu_n}{\mu_f} = \frac{1}{(1-\varphi)^{2.5}}$$

$$k^* = \frac{k_n}{k_f} = \frac{[k_p + 2k_f - 2(k_f - k_p)\varphi]}{[k_p + 2k_f + 2(k_f - k_p)\varphi]}$$

The solution procedure of the discretized equations is based on a line-by-line iteration method in the axial and radial directions using Fortran Power Station program. The solution procedure of the numerical analysis which performed in the above separated region is as follows:

1- Calculate saturation temperature using equation (34).

2- Calculate velocity and temperature boundary condition at the vapor-liquid interface using equations (5) and (6).

3- Solve the equations of stream function and vorticity in vapour and liquid regions sequentially based on the velocities obtained in step 2 and the values of stream function and vorticity at the boundaries where the boundary conditions are applied.

4- Calculate the velocity components (u and v) by using the current values of stream function and the values at boundaries.

5- Solve the momentum equations in x-direction for vapour region and wick structure using the current values for velocities.

6- Solve the energy equations in vapour, liquid and wall regions sequentially by using the current values of stream function and the values at boundaries.

the above procedure repeated until the convergence is achieved with relative error for the calculated parameters (ψ, ω, p and θ) equal to $5 * 10^{-5}$. **Fig 2** illustrates the flow chart for the current computer program in the present study.

4. RESULTS AND DISCUSSION

The analysis of a cylindrical horizontal heat pipe was carried out by incorporating the effect of water based nanofluid, namely Al_2O_3, in the present numerical model. 1, 3 and 5 Vol.% concentration are chosen for particle size of 35nm. The performance of the heat pipe is investigated for different heat inputs. In which, the influence of nanofluid on liquid pressure drop, axial velocity, radial velocity, stream function, temperature difference, thermal resistance, maximum heat transport capability and capillary pressure is investigated. The specifications of the heat pipe are shown in **table 1**.

As seen in, the dimensionless contours plot, **fig.s 3 – 14**. For the same heat input, the liquid pressure and stream line inside the heat pipe decreases when increasing the nanoparticle concentration (NPC). This is due to an increase in the fluid density in the presence of more nanoparticles, as can be seen in equation (17). As a result of this increase in the nanofluid density, a slower liquid flow is observed.

For the same nanoparticle concentration, when the heat transfer rate increase the mass flow rate increased so that the fluid velocities increased, which lead to increase the liquid pressure and stream line values. Also, due to increasing the heat transfer rate the saturation pressure will increase, which in turn lead to increase the heat pipe operation temperature.

Fig. 15 show the effect of particle concentration levels on the temperature difference between evaporator and condenser for various heat loads. The figure shows that increasing the particle concentration decreases the temperature difference between the evaporator and condenser.

The maximum heat transport capillary limit and the capillary pressure as function of particles concentration can be seen in **fig. 16**. Increasing the nanoparticle concentration enhances the maximum heat transfer and the capillary pressure. This is due to an increase in the latent heat of vaporization and the surface tension with the nanoparticle concentration, as can be seen in equations (19 and 20).

Fig. 17 show the influence of different nanoparticle concentration levels on the heat pipe thermal resistance under different heat input. It can be seen that increasing the nanoparticle concentration decreases the heat pipe thermal resistance and provides a better performance. For example, the percentage enhancement in R_{th} reaches up to 35.3% at heat transfer rate of 30W and NPC = 0.05 compared to its value when using pure water.

To verify the current numerical model of the heat pipe. the result of wall temperature distribution along the heat pipe is compared with the result of (Do et al., 2010) for the similar problem. **Fig. 18** show a good agreement for the temperature distribution at 3 watt as transmitting heat power and NPC of 0.01.

5. CONCLUSION

This paper deals with the thermal enhancement of the heat pipe performance, using Alumina – nanofluid as the working fluid. In the present work, the DI-water with Alumina nanoparticles, for three concentration levels 1, 3 and 5 Vol.%, in heat pipe was numerically simulated using Fortran Power Station Program.

Conclusions may be drawn from the results of the numerical model as follows:

- The dimensionless parameters (liquid pressure, Uvelocity, Vvelocity, stream function and temperature distribution) of the heat pipe with nanofluid is lower than that with DI-water.
- The more Alumina nanoparticles in the working fluid enhancement of the heat pipe performance expressed by of the performance curves (the temperature difference versus heat transfer rate).

- The maximum heat transfer rate and the capillary pressure increases as the nanoparticle concentration increases.
- The thermal resistance of the heat pipe with nanofluid is lower than that with DI-water. It is shown that the thermal resistance decreases as the concentration level increases.
- Results indicate that the Alumina nanofluid has remarkable potential as working fluid for horizontal heat pipe of higher thermal performances.

6. REFRENCESS

[1] Borujerdi A. N., Layeghi M., "A Numerical Analysis of Vapor Flow in Concentric Annular Heat Pipes", Transaction of ASME: Journal of Fluids Engineering, Vol. 126, pp.442- 448, 2004.

[2] Do K. H., Ha H. J. and Jang S. P., "Thermal resistance of screen mesh wick heat pipes using the water-based Al_2O_3 nanofluids", International Journal of Heat and Mass Transfer 53 (2010) 5888–5894.

[3] Do K.H. and Jang S.P., "Effect of nanofluids on the thermal performance of a flat micro heat pipe with a rectangular grooved wick", International Journal of Heat and Mass Transfer 53 (2010) 2183–2192.

[4] Fadhil O. T., "Numerical and Experimental Study on a Heat Pipe With Porous Media Wick", Ph.D. Thesis, university of Technology, 2006.

[5] Ferrouillat S., Bontemps A., Ribeiro J.P., Gruss J.A. and Soriano O., "Hydraulic and heat transfer study of SiO_2/water nanofluids in horizontal tubes with imposed wall temperature boundary conditions", International Journal of Heat and Mass Transfer 32 (2011) 424–439.

[6] Hajian R., Layeghi M. and Sani K. A., "Experimental study of nanofluid effects on the thermal performance with response time of heat pipe", Energy Conversion and Management 56 (2012) 63–68.

[7] Jiji Latif M. , Heat Convection, © Springer 2006.

[8] Kang S.W., Wei W.C., Tsai S.H. and Huang C.C., "Experimental investigation of nanofluids on sintered heat pipe thermal performance", Applied Thermal Engineering 29 (2009) 973–979.

[9] Kang S.W., Wei W.C., Tsai S.H. and Yang S.Y., "Experimental investigation of silver nanofluid on heat pipe thermal performance", Applied Thermal Engineering 26 (2006) 2377–2382.

[10] Liu Z.H. and Zhu Q.Z., "Application of aqueous nanofluids in a horizontal mesh heat pipe", Energy Conversion and Management 52 (2011) 292–300.

[11] Mahjoub S., Mahtabroshan A., "Numerical Simiulation of a Conventional Heat Pipe", World Academy of Science, Engineering and Technology, Vol. 39, pp. 117-122, 2008.

[12] Mousa M.G., "Effect of nanofluid concentration on the performance of circular heat pipe", Ain Shams Engineering Journal 2 (2011), 63–69.

[13] Naphon P., Assadamongkol P. and Borirak T., "Experimental investigation of titanium nanofluids on heat pipe thermal efficiency", International Communications in Heat and Mass Transfer 35 (2008), 1316–1319.

[14] Peterson G.P., "An Introduction to Heat Pipes: Modeling", Testing, and Applications, John Wiley & Sons, New York, 1994.

[15] Rashidian B., Amidpour M. and Jafari Nasr M. R., "Modeling the Transient Response of the Thermosyphon Heat Pipes", Proceedings of the World Congress on Engineering, Vol. II, London, U.K., 2008.

[16] Reay D. and Kew P., Heat Pipes: Theory, Design and Applications, Fifth Edition,Elsevier, 2006.
Cleary M., Grimes R., Hodes M. and North M. T., "Design of a Variable Conductance Heat Pipe for a Photonic Component", Proceedings of IMECE2006 , Chicago, USA, 2006.

[17] Shafahi M., Bianco V., Vafai K. and Manca O., "An investigation of the thermal performance of cylindrical heat pipes using nanofluids", International Journal of Heat and Mass Transfer 53 (2010) 376–383.

[18] Shahi M., Mahmoudi A.H. and Talebi F., "Numerical simulation of steady natural convection heat transfer in a 3-dimensional single-ended tube subjected to a nanofluid", International Journal of Heat and Mass Transfer 37 (2010) 1535–1545.

[19] Solomon A. B., Ramachandran K., Pillai B.C., "Thermal performance of a heat pipe with nanoparticles coated wick", Applied Thermal Engineering 36 (2012) 106-112.

[20] Sreenivasa T. N., Sridhara S.N. and Pundarika G., "Working Fluid Inventory in Miniature Heat Pipe", Proceedings of the International Conference on Mechanical Engineering, Dhaka, Bangladesh, 2005.

[21] Tsai C.Y., Chein H.T., Ding P.P., Chan B., Luh T.Y. and Chen P.H., "Effect of structural character of gold nanoparticles in nanofluid on heat pipe thermal performance". Materials Letters. 58 (2004), 1461–1465.

[22] Wang P.Y., Chen X.J., Liu Z.H., Liu Y.P., "Application of nanofluid in an inclined mesh wicked heat pipes", Thermochimica Acta (2012) 1-36.

[23] Zhu N. and Vafai K., "Analysis of cylindrical heat pipes incorporating the effects of liquid–vapor coupling and non-Darcian transport–a closed form solution", International Journal of Heat and Mass Transfer 42 (1999) 3405–3418.

Table 1: Heat pipe specification.

Heat pipe container material	copper
Wall thickness	0.85mm
Outer diameter	19.05mm
Heat pipe length	555mm
Evaporator length	150mm
Condenser length	97mm
Working fluid	DI water and Al_2O_3 nanofluid
Sink temperature	22 ^oC
Set temperature	100 ^oC

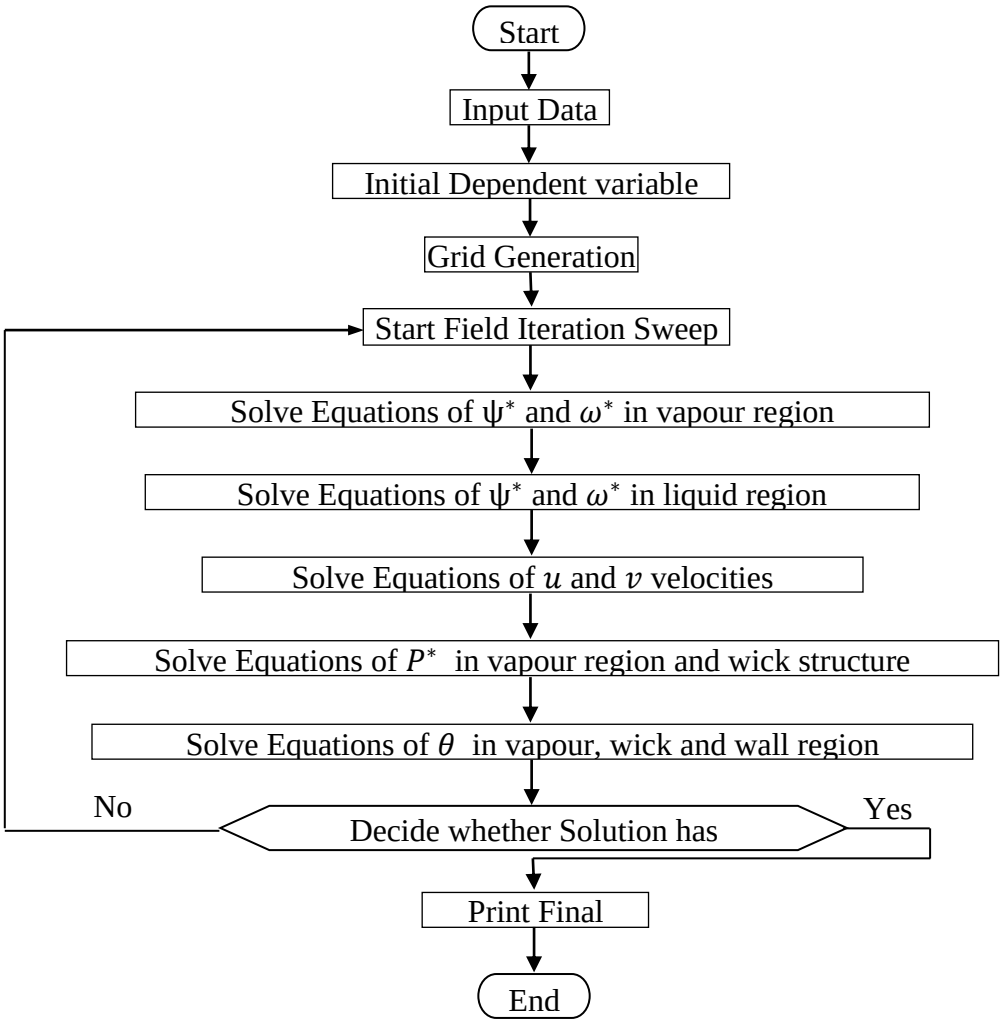

Figure 2: Flow chart for the current computer program.

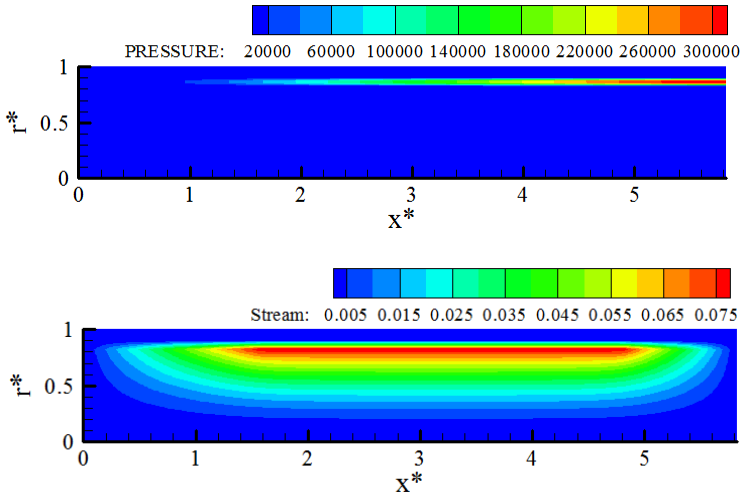

Figure 3: Dimensionless liquid pressure and Stream line distribution inside the heat pipe at Q_{in}=10 W and φ=0.

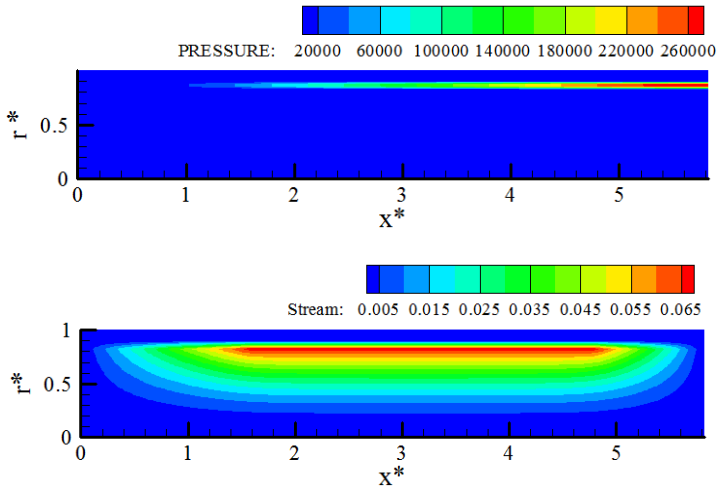

Figure 4: Dimensionless liquid pressure and Stream line distribution inside the heat pipe at Q_{in}=10 W and φ=0.01.

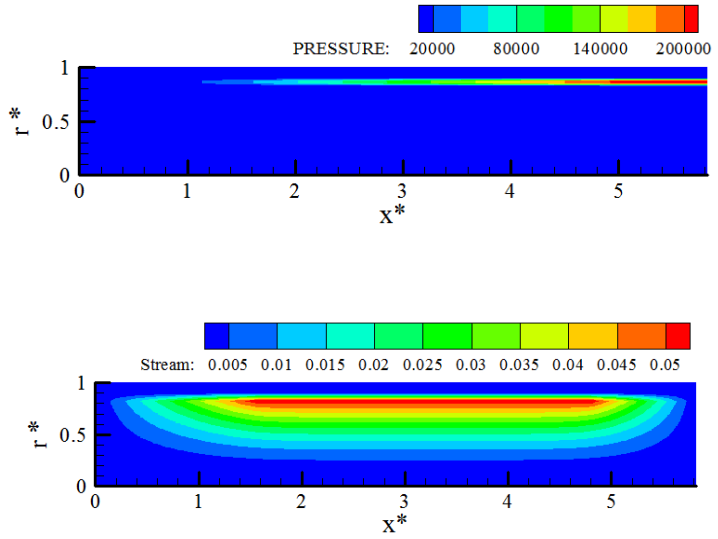

Figure 5: Dimensionless liquid pressure and Stream line distribution inside the heat pipe at Q_{in}=10 W and φ=0.03.

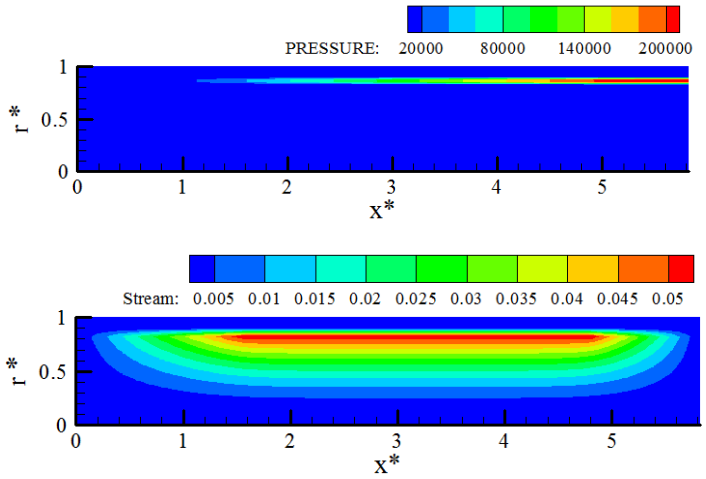

Figure 6: Dimensionless liquid pressure and Stream line distribution inside the heat pipe at Q_{in}=10 W and φ=0.05.

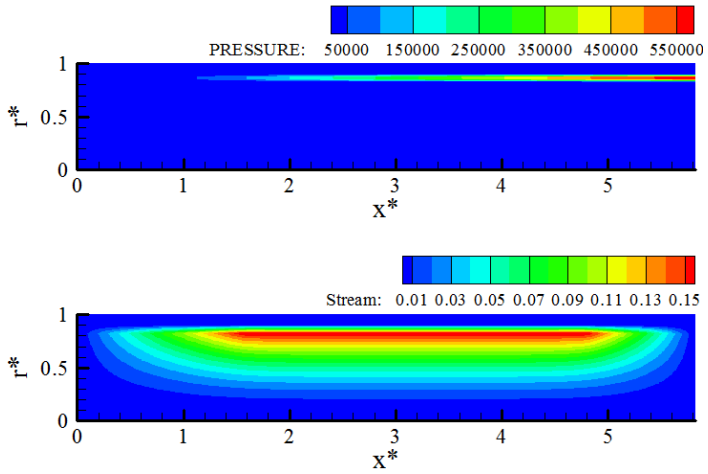

Figure 7: Dimensionless liquid pressure and Stream line distribution inside the heat pipe at Q_{in}=20 W and φ=0.

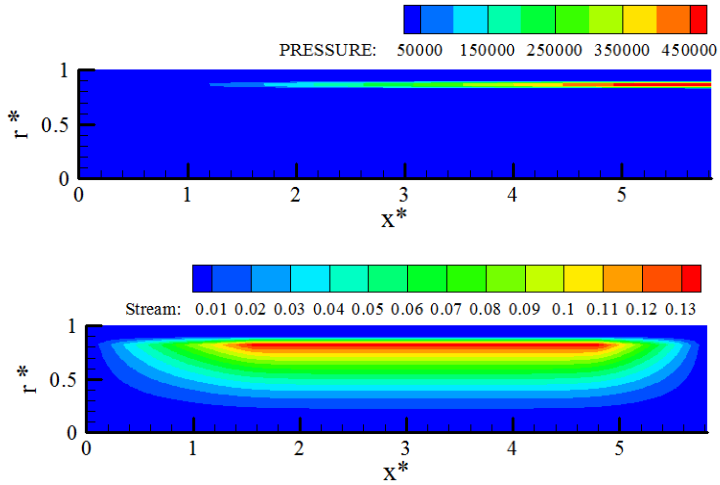

Figure 8: Dimensionless liquid pressure and Stream line distribution inside the heat pipe at Q_{in}=20 W and φ=0.01.

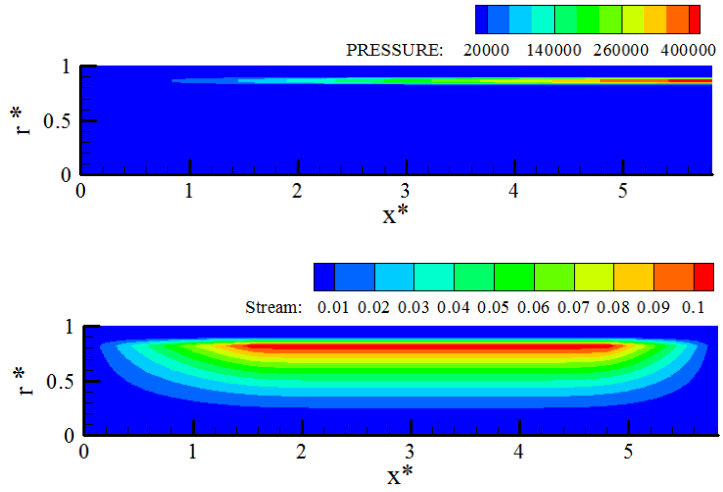

Figure 9: Dimensionless liquid pressure and Stream line distribution inside the heat pipe at Q_{in}=20 W and φ=0.03.

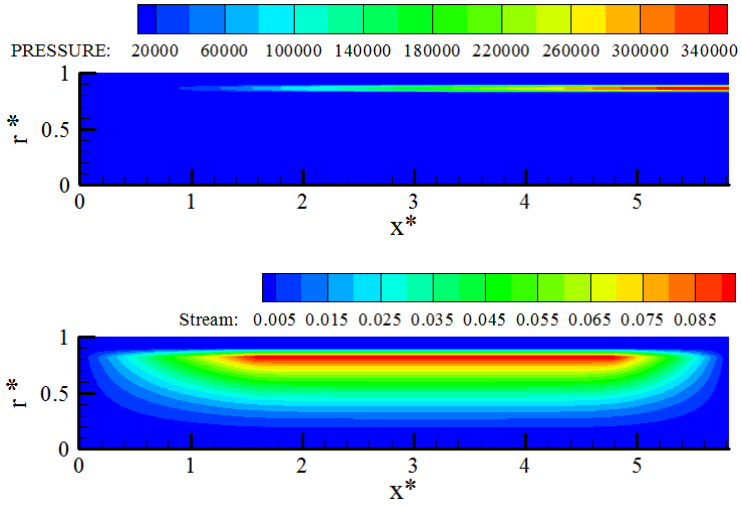

Figure 10: Dimensionless liquid pressure and Stream line distribution inside the heat pipe at Q_{in}=20 W and φ=0.05.

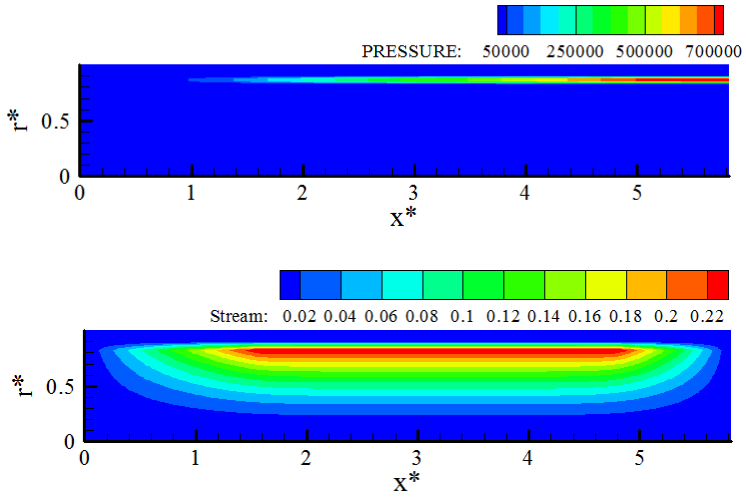

Figure 11: Dimensionless liquid pressure and Stream line distribution inside the heat pipe at Q_{in}=30 W and φ=0.

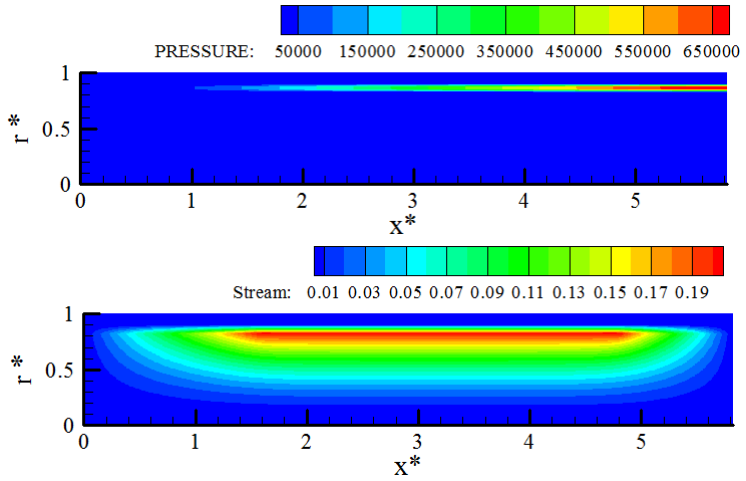

Figure 12: Dimensionless liquid pressure and Stream line distribution inside the heat pipe at Q_{in}=30 W and φ=0.01.

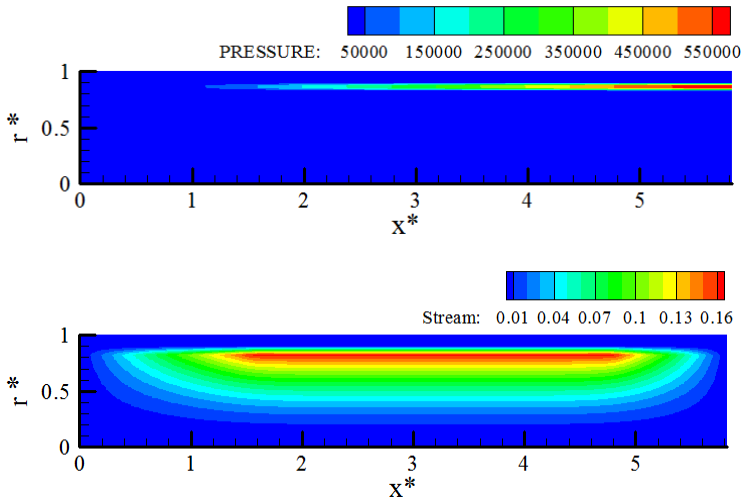

Figure 13: Dimensionless liquid pressure and Stream line distribution inside the heat pipe at Q_{in}=30 W and φ=0.03.

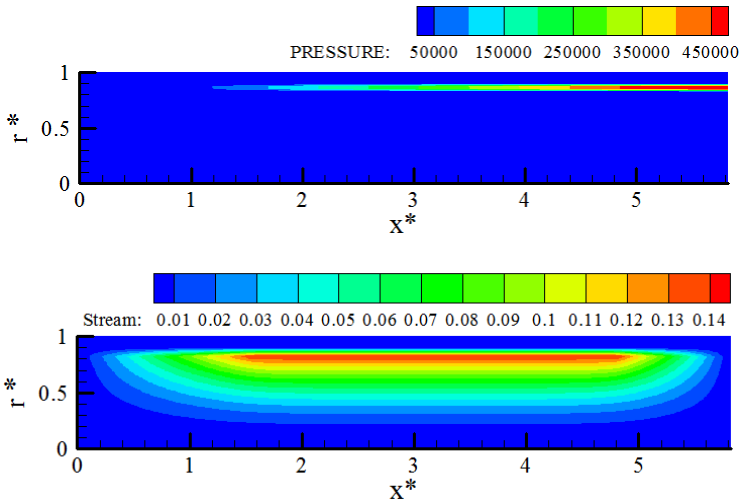

Figure 14: Dimensionless liquid pressure and Stream line distribution inside the heat pipe at Q_{in}=30 W and φ=0.05.

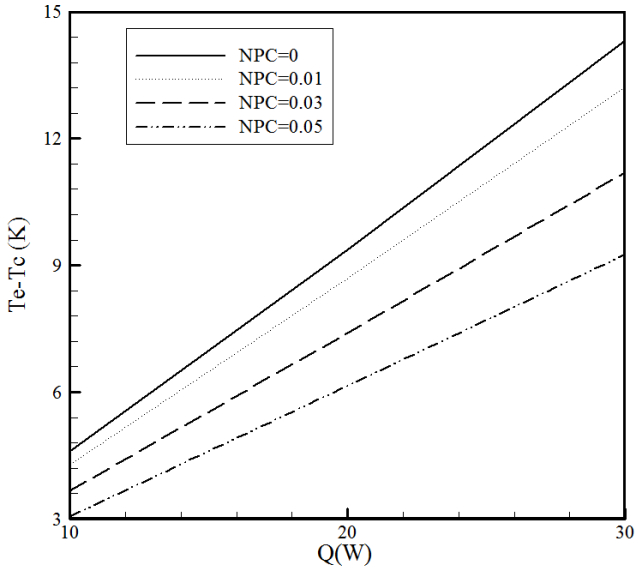

Figure 15: Effect of particle concentration levels on the thermal performance of a heat pipe under various heat input.

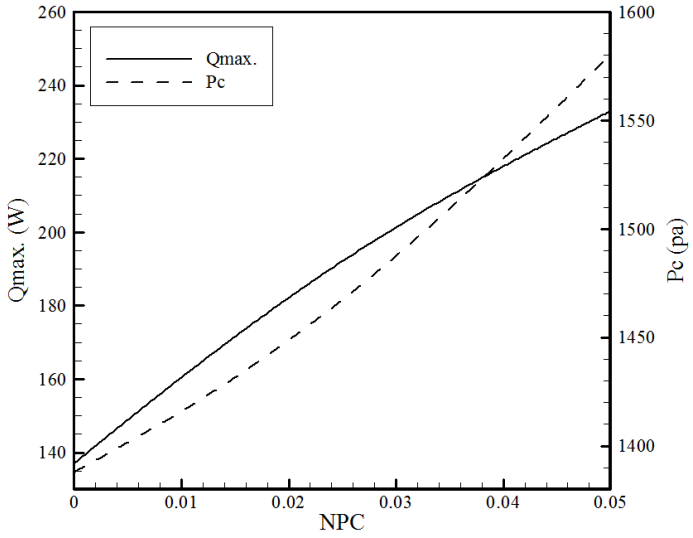

Figure 16: The effect of nanoparticles concentration levels on the maximum heat transfer limit and capillary pressure of the heat pipe.

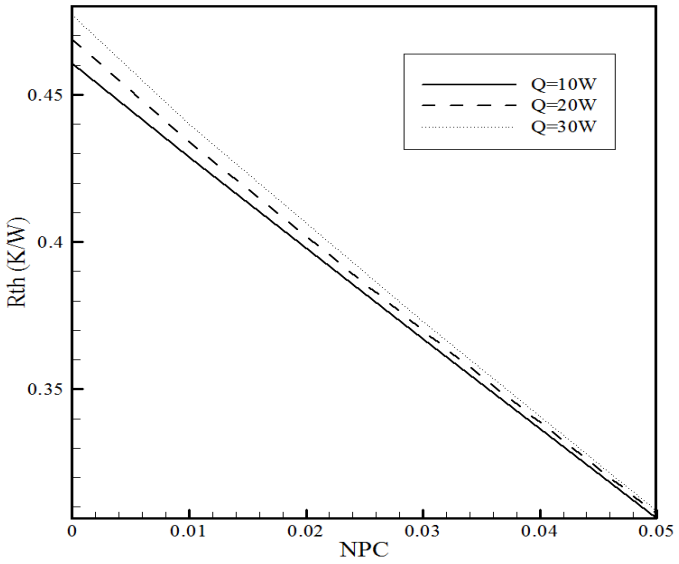

Figure 17: The effect of different nanoparticle concentration levels on the heat pipe thermal resistance.

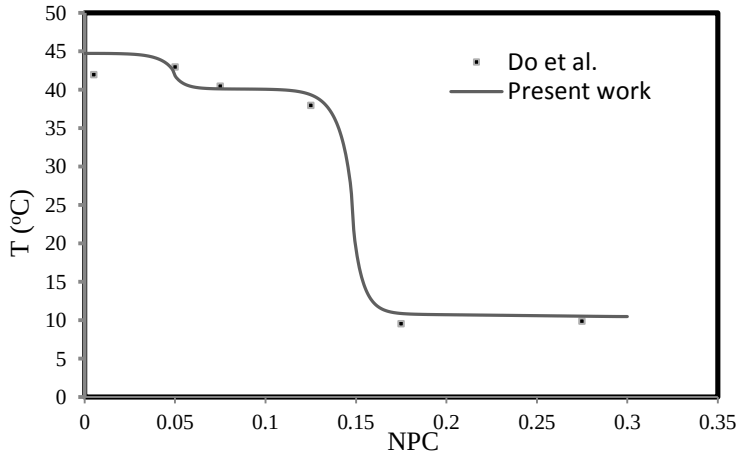

Figure 18: Comparing current model with available numerical data.